ISSN 0024-4902, Lithology and Mineral Resources, 2015, Vol. 50, No. 2, pp. 102–116. © Pleiades Publishing, Inc., 2015.
Original Russian Text © A.V. Soloviev, A.V. Zaionchek, O.I. Suprunenko, H. Brekke, J.I. Faleide, D.V. Rozhkova, A.I. Khisamutdinova, N.M. Stolbov, J.K. Hourigan, 2015, published in Litologiya i Poleznye Iskopaemye, 2015, No. 2, pp. 113–128.

Evolution of the Provenances of Triassic Rocks in Franz Josef Land: U/Pb LA-ICP-MS Dating of the Detrital Zircon from Well Severnaya

A. V. Soloviev[a, f], A. V. Zaionchek[a, b], O. I. Suprunenko[b], H. Brekke[c], J. I. Faleide[d], D. V. Rozhkova[a], A. I. Khisamutdinova[a], N. M. Stolbov[b], and J. K. Hourigan[e]

[a]*Geological Institute, Russian Academy of Sciences, Pyzhevskii per. 7, Moscow, 119017 Russia*
e-mail: fission-track@mail.ru
[b]*All-Russia Research Institute of Geology and Mineral Resources of the World Ocean, Angliiskii pr. 1, St. Petersburg, 190121 Russia*
[c]*Norwegian Petroleum Directorate, Stavanger, Norway*
[d]*University of Oslo, Oslo, Norway*
[e]*Department of Earth and Planetary Sciences, University of California, Santa Cruz, 1156 High Street, Santa Cruz, California, 95064, U.S.A.*
[f]*Rosgeologiya OJSC, ul. Khersonskaya 43/3, Moscow, 117246 Russia*
Received April 8, 2013

Abstract—Morphological analysis and U/Pb LA-ICP-MS dating were carried out for detrital zircon (400 age determinations) from four core samples of Triassic rocks recovered by Well Severnaya (Graham Bell Island, Franz Josef Land Archipelago). It is shown that source areas were mainly composed of peraluminous granites. U/Pb LA-ICP-MS zircon data were used to decipher the provenance evolution in the northern Barents Sea region. The main source of clastic material in the North Barents sedimentary basin in the Middle–Late Triassic was the Uralian fold belt, with lesser contribution from the East European Craton (Baltica), Timanides, Taimyr, and rocks related to the Siberian plume. The clastic material was mainly transported from the south and southeast. From the beginning of the Middle to the terminal Late Triassic, influence of the Neoproterozoic sources systematically decreased, whereas contribution of Caledonian sources increased.

DOI: 10.1134/S0024490215020054

INTRODUCTION

The Franz Josef Archipelago is one of the key objects for reconstructing the history of the Triassic sedimentation in the North Barents Sea region (Fig. 1). This study has a great scientific and applied significance in relation with the presence of considerable hydrocarbon reserves in the Barents Sea. Reconstruction of the age and composition of the provenance of clastic material for the Arctic Triassic rocks is an urgent problem hotly debated during the last decade (Miller et al., 2006; Pease et al., 2007; Petrov, 2010; Bue et al., 2011; Omma et al., 2012; Miller et al., 2013; Bue and Andersen, 2013). Single-grain dating with precision geochronological methods offers new opportunities for studying terrigenous rocks. Zircon is widespread in detrital rocks, being resistant to weathering and decomposition. Individual grains of detrital zircon are dated by U/Pb LA-ICP-MS (Gehrels, 2011; and others). Their morphology bears important information on provenances (Zircon, 2003), while typomorphism (Pupin, 1980; Belousova et al., 2006) provides insight into physicochemical conditions (temperature, pressure, agpaitic index) of the formation of eroded complexes. In this work, the age, typomorphism, and the inner structure of detrital zircon are studied to decipher the provenances and regional paleogeographic setting.

TRIASSIC ROCKS OF THE BARENTS SEA REGION

The study of the Arctic shelf has recently received great attention. Mesozoic rocks within the Barents Sea Region have been studied sufficiently well from parametric and marine drilling data (Gramberg et al., 1985; Bro et al., 1989). The Triassic terrestrial rocks were studied onland in the Svalbard Archipelago (Pchelina, 1985, Mørk, 1999), Medvezhii and Nadezhda Islands (Pchelina, 1985), western Novaya Zemlya Archipelago (Ustritskii, 1981), as well as in the parametric boreholes on the Franz Josef Land (Preobrazhenskaya et al., 1985). Triassic rocks of the Norwegian Barents Sea were studied in marine boreholes (Bugge and Fanavoll, 1995; Mørk, 1999). Thickness of the Triassic rocks varies from 690 to over 3800 m (Basov et al., 2009). Within the Barents Sea region, the

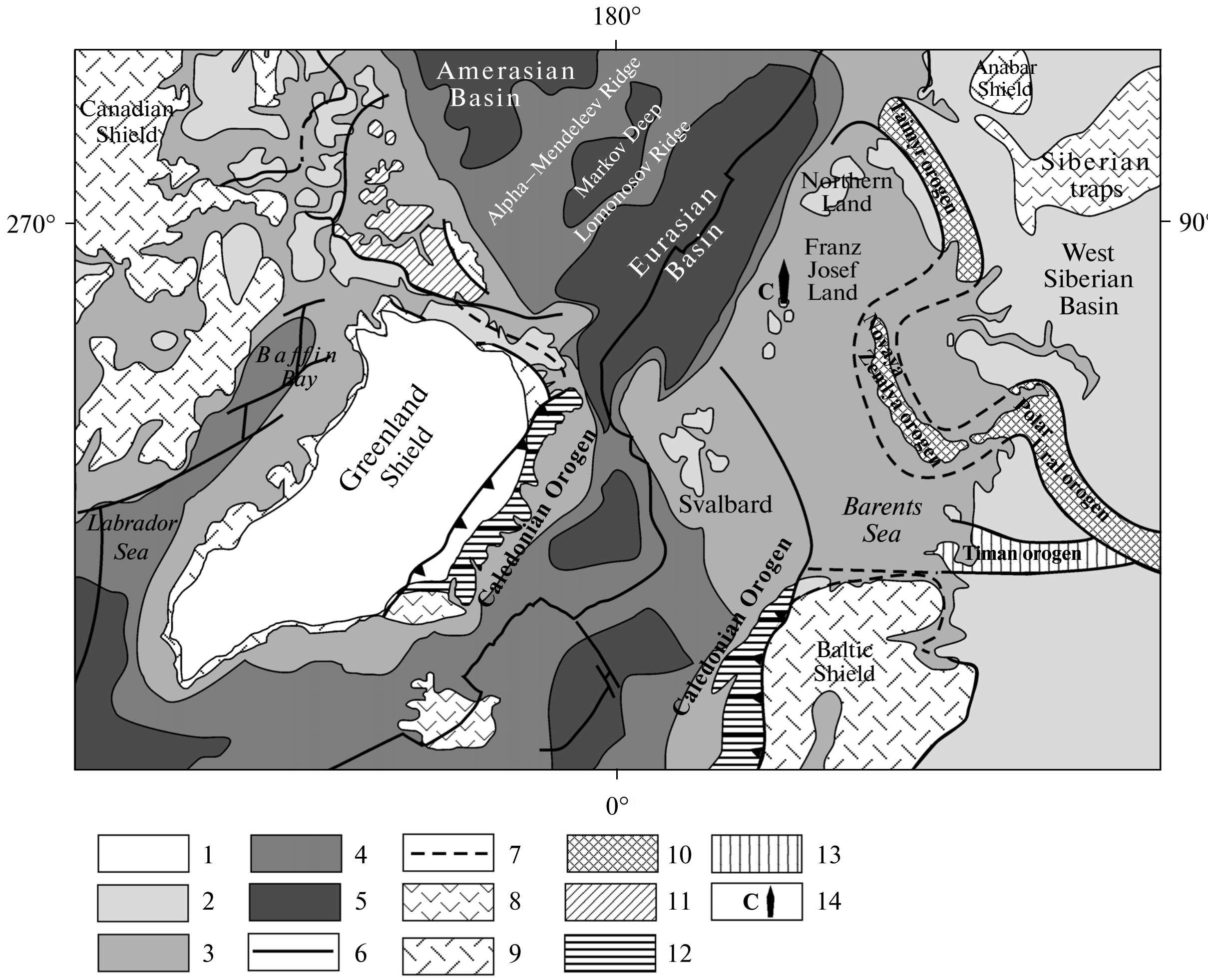

Fig. 1. Tectonic scheme of the West Arctic region (Omma et al., 2011). (1) Greenland glaciers; (2) land; (3–5) sea depth, m: (3) 0–400, (4) 400–3500, (5) >3500; (6) tectonic boundaries; (7) inferred tectonic boundaries; (8) fields of basalts and volcanic belts (≤252 Ma); (9) Precambrian shields; (10–13) orogens: Late Paleozoic–Early Mesozoic Hercynian (Uralian); (11) Early Paleozoic Ellesmirian; (12) Early Paleozoic Caledonian; (13) Neoproterozoic–Cambrian Timan; (14) position of Well Severnaya in Graham Bell Island, Franz Josef Land Archipelago.

Triassic rocks are represented by terrigenous rocks of different facies with carbonate interbeds and nodules.

In the 1970s, islands of Franz Josef Land were studied by three parametric boreholes: Nagurskaya, Severnaya, and Hayes (Gramberg et al., 1985). Well Severnaya reached a depth of 3523 m in Graham Bell Island of the Franz Josef Archipelago, but did not leave Triassic rocks (Preobrazhenskaya et al., 1985; Dypvik et al., 1998). Well Severnaya recovered the Upper and Middle Triassic rocks (Figs. 1, 2). The Upper Triassic sequence comprises the Norian and Raethian clayey–aleuritic sediments and Carnian mainly sandy––aleuritic sediments intercalated with coaly rocks and lenses of bituminous coal (Gramberg et al., 1985). The Middle Triassic sequence is dominated by Ladinian and Anisian alueritic–clayey sediments. The borehole recovered six intrusive bodies from 5 to 87 m thick (Fig. 2). The igneous rocks are represented by dolerites, microdolerites, micropegmatite gabbro, and olivine gabbrodolerites (Gramberg et al., 1985). The presence of sandstones at different stratigraphic levels in the borehole section (Fig. 2) allowed us to collect samples for the heavy fraction analysis and the detailed study of detrital zircon grains. Core samples were taken from different depths and stratigraphic levels (Fig. 2).

Sample C2688 was taken from the Middle Triassic (upper Anisian) sandstones at a depth of 2688 m; sample C2073 (sandstone) was taken from Middle Triassic (upper Ladinian) detrital rocks at a depth of 2073 m; sample C1040 was collected from Late Triassic (upper Carnian) psammites at a depth of 1040 m (Preobrazhenskaya et al., 1985; Dypvik et al., 1998); and sample C633 (aleurosandstones) with the inferred Upper Triassic (upper Norian) age was taken at a depth of 633 m.

The samples are medium- to coarse-grained polymictic sandstones corresponding to feldspar–

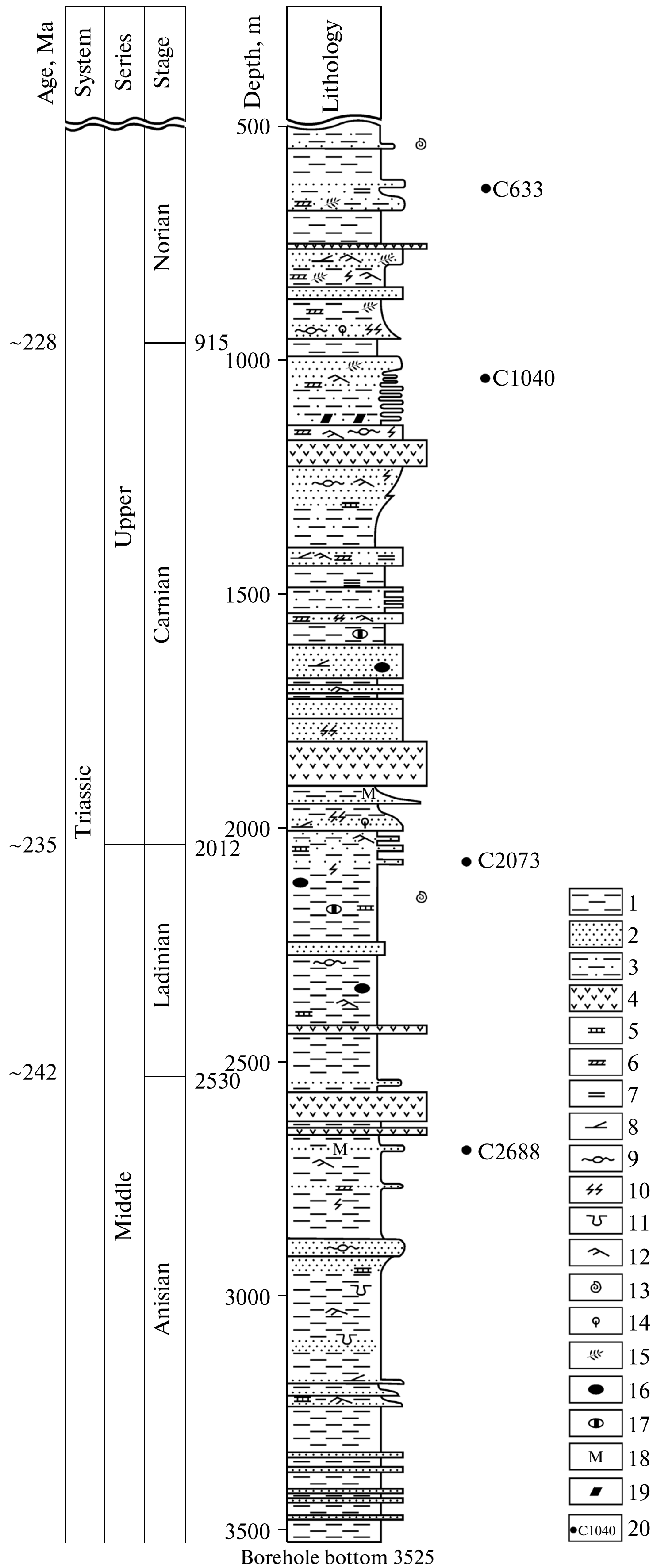
Age, Ma
System
Series
Stage
Depth, m
Lithology
~228
~235
~242
Triassic
Upper
Middle
Norian
Carnian
Ladinian
Anisian
915
2012
2530
500
1000
1500
2000
2500
3000
3500
M
•C633
•C1040
• C2073
• C2688
1
2
3
4
5
6
7
8
9
10
11
12
13
14
15
16
17
18
19
•C1040
20
Borehole bottom 3525

Fig. 2. Fragment of Well Severnaya section, Franz Josef Land Archipelago. Modified after (Preobrazhenskaya et al., 1985; Dypvik et al., 1998). (1–4) Rocks: (1) argillites, (2) sandstones, (3) aleurolites, (4) igneous; (5, 6) matrix: (5) calcitic, (6) dolomitic; (7–12) structures: (7) laminated, (8) cross-bedded, (9) hummocky cross-bedded; (10) bioturbation traces; (11) loading structure, (12) ripple marks; (13) fauna, (14) plant detritus; (15) plant remains; (16, 17) nodules: (16) pyrite, (17) siderite; (18) mica; (19) coal; (20) number of samples collected for the analysis of detrital zircon.

quartz (sample C2688) and quartz–feldspar graywackes (sample C1040). They are made up of quartz (30–40%), feldspars (25–35%), rock fragments (15–40%), mica (5%), organic matter (5%), and accessory minerals. Quartz forms both rounded and irregularly shaped grains with corroded boundaries. The prevailing monocrystalline quartz has a straight, more rarely undulose extinction, while the less common poorly rounded polycrystalline quartz displays undulose and mosaic extinction. Feldspars are plagioclase and microcline. Their crystals have a tabular, rarely equant, habit. There are also twinned crystals and grains with clearly expressed microcline cross-hatching, as well as scarce intergrowths of feldspar and quartz. Rock fragments are represented by quartzites with typomorphic microcrystalline appearance, felsitic volcanic rocks, and devitrified glass. The volcanic rocks and glass usually experienced secondary alteration, being replaced by fine-scale clayey aggregate. Biotite and muscovite occur as weakly bent altered flakes up to 0.7 mm long. They are localized in the interstices, enveloping quartz and feldspar. Accessory minerals are represented by rounded and prismatic zircon. Matrix accounts for 10–20% of polished thin section area and has a mixed composition. Carbonate replacement matrix is developed after plagioclase. In general, sandstones have a clayey–carbonate matrix with locally developed zones consisting of small fragments of plagioclase, quartz, clay minerals, carbonate, and devitrified volcanic glass. The matrix is porous and contoured and shows a patchy distribution in the rock.

Thin-bedded aleurosandstone (sample C633) is made up of quartz (85%), feldspars (7%), altered rock fragments (5%), and muscovite (3%). Quartz is represented by weakly rounded or less common rounded monocrystalline grains with straight extinction. The grains are practically devoid of gas–liquid inclusions and fractures. Polycrystalline quartz is absent. Feldspars are mainly represented by tabular (95%) untwinned unaltered plagioclase and rare micrcoline. Weakly deformed muscovite flakes with high interference color and clear cleavage fractures are often oriented parallel to bedding. Accessory minerals are represented by rare zircon grains. Rock fragments presumably represent volcanic glass. Matrix occupies 40% of polished thin section area and consists of clayey–carbonate aggregate, (locally, secondary chlorite) with uneven patchy distribution of organic material. Bedding is caused by uneven banded distribution of clay material. Aleurosandstone is cemented by mixed matrix: continuous uneven, open porous, and locally, basal.

METHODS AND RESULTS

Heavy Fraction Minerals

Heavy fraction minerals were extracted using conventional technique at the Laboratory of Mineralogi-

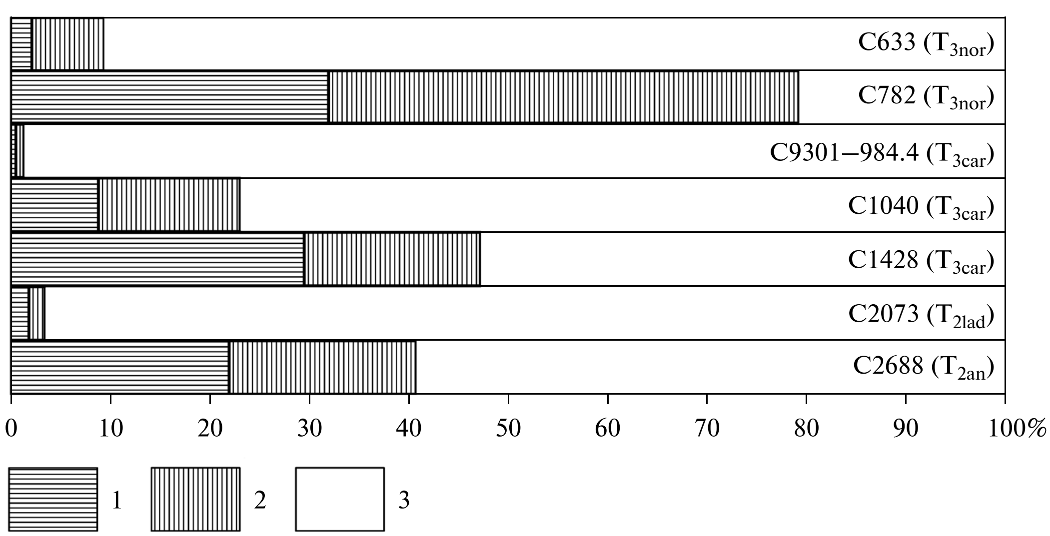

Fig. 3. Distribution of heavy fraction minerals in sandstones from Well Severnaya. Indicator minerals of source areas: (1) sialic rocks (zircon, apatite, rutile, and tourmaline); (2) mafic rocks (spinel, ilmenite, leucoxene); (3) cosmopolitan minerals (anatase, brookite, garnet, monazite, magnetite, sulfides, sphalerite, staurolite, amphibole, chlorite, mica, carbonate, iron hydroxides, biotite).

Table 1. Analysis of heavy fraction minerals in sandstones from Well Severnaya, Franz Josef Land Archipelago

Sample no.*	Sample weight (g)	Heavy fraction weight (mg)	Heavy fraction output (%)	Mineral content (%) in the heavy fraction																				
				Zircon	Apatite	Rutile	Anatase	Brookite	Leucoxene	Garnet	Monazite	Spinel	Tourmaline	Ilmenite	Magnetite	Sulfides	Sphalerite	Staurolite	Amphibole	Chlorite	Mica	Carbonate	Iron hydroxides	Biotite
C633	830	10581.1	1.27	0.95	0.06	0.63	0.01	0.07	2.99	0.83	–	1.46	0.37	3.05	0.18	2.55	–	0.39	–	–	–	83.89	2.58	–
C782	1485	398.1	0.03	13.69	2.41	12.06	0.38	–	18.34	18.46	–	19.84	3.77	9.04	–	–	–	–	–	–	–	–	2.01	
C930.1–941.4	800	2051.0	0.26	0.22	0.26	0.10	0.01	0.02	0.75	0.02	–	0.07	0.05	–	–	0.01	–	–	0.01	–	–	–	98.49	
C1040	670	1206.5	0.18	3.58	2.86	1.48	0.03	0.17	10.03	7.63	–	4.23	0.97	–	–	0.12	–	–	–	1.36	–	–	67.55	
C1428	570	1012.5	0.18	8.26	13.73	5.37	0.86	–	13.04	5.19	–	4.59	2.04	–	–	–	–	–	–	1.21	45.43	–		0.28
C2073	1500	4988.3	0.33	0.33	0.72	0.46	0.01	–	1.35	0.35	–	0.25	0.37	–	–	3.75	0.04	–	–	0.16	88.21	–	4.01	
C2688	550	1631.6	0.30	6.74	1.84	9.07	0.01	3.68	17.34	24.33	0.10	1.52	4.24	–	–	0.92	–	–	–	15.44	–	–	14.77	

* Sample number corresponds to the sampling depth. Dash denotes mineral was not found.

Table 2. Content (%) of zircons of different morphological types (Pupin, 1980) in the core from Well Severnaya (Franz Josef Land Archipelago)

Sample no.*	Age	Morphological type																*N*
		H	L1	L3	L4	G1	I	Q2	S6	S7	S9	S15	S19	S21	S22	S24	S25	
C2688	T_2 (upper Anisian)	12.7	24.1	5.4	11.3	0.0	0.0	0.0	5.4	6.7	12.7	9.4	0.7	0.0	1.3	2.9	7.4	149
C2073	T_2 (upper Ladinian)	9.4	22.6	2.2	2.9	0.0	1.4	3.6	7.3	8.0	9.4	8.7	0.0	1.4	4.3	2.9	15.9	138
C1040	T_3 (upper Carnian)	17.1	25.0	7.8	9.4	0.0	0.0	0.0	3.1	0.0	25.0	6.3	1.6	0.0	3.1	0.0	1.6	64
C633	T_3 (upper Norian)	11.2	24.4	0.7	14.0	1.4	0.0	1.4	8.4	7.0	11.2	7.0	1.4	1.4	2.1	1.4	7.0	143

* Sample number corresponds to the sampling depth in a well. N is the number of calculated grains. Designations of morphological types correspond to united fields: H = H + Q1, L1 = L1 + L2 + S1 + S2, L3 = L3 + S3, L4 = L4 + L5+S4 + S5, G1 = G1 + P1, I = I + R1, Q2 = Q2 + Q3, S6 = S6 + S11, S7 = S7 + S8 + S12 + S13, S9 = S9 + S10 + S14, S15 = S15 + P3 + S20 + P4, S19 = S19, S21 = S21 + J1, S22 = S22 + S23 + J2 + J3, S24 = S24 + J4, S25 = S25 + P5 + J5 + D.

cal and Track Analysis of the Geological Institute, Russian Academy of Sciences. The examination of heavy fraction revealed a wide range of minerals (Table 1, Fig. 3). The minerals are grouped into indicators of sialic rocks (zircon, apatite, rutile, and tourmaline); mafic rocks (spinel, ilmenite, leucoxene); and cosmopolitans (anatase, brookite, garnet, monazite, magnetite, sulfides, sphalerite, staurolite, amphibole, chlorite, mica, carbonate, iron hydroxides, and biotite). The obtained data did not allow us to reveal a clear trend or the predominance of a definite provenance. Samples C782, C1428, and C2688 contain significant amounts of minerals that are typical of felsic and basic rocks (in equal proportions). Some samples (C633, C 930-941.4, C1040) comprise a large amount of secondary minerals: siderite (C633) and iron hydroxide (C930—941.4, C1040), which indicate a high degree of rock transformation.

Morphology of Detrital Zircons

Only euhedral zircons (10–30% of all zircons) were morphologically analyzed and calculated. Calculations were carried out using a Meiji ZOOM RZ-B series stereomicroscope, which provides a high-resolution sharp image undistorted under magnification up to 300. For convenience in calculation, we modified the zircon classification (Pupin, 1980). The distinguished groups included morphological types with similar structure without allowance for the elongation coefficient. Each of the groups was termed according to the left morphological type in the classification (Pupin, 1980) (Table 2, Fig. 4).

Sample C2688 comprises colorless, light pink, and yellowish pink zircon. Some grains are "fused" and have corroded surface, but the majority of zircon are characterized by even lustrous faces. Accumulations of small inclusions observed in some grains impart grayish color to the mineral. Individual crystals contain intergrowths of brown-black acicular rutile (?). Euhedral particles account for 20–30% of all zircon grains (Table 2, Fig. 4a).

Sample C2073 contains colorless, pale yellow, and pale pink zircon. Grains of volcanic origin (2 to 3%) have elongation coefficient of 3–5. They are colorless and pale yellow, without visible inclusions. There are also scarce transparent zircons with vague cores. Some crystals contain inclusions of black, sometimes acicular, mineral (probably rutile). Euhedral grains account for 10–15% (Table 2).

Sample C1040 contains a few zircon grains. Therefore, only a limited number of grains were used for calculation (Table 2).

Sample C633 contains transparent zircon, with the predominance of pale yellow, yellow, and pale orange grains. Colorless zircon is rare. The crystals host dust inclusions of black mineral. Euhedral grains account for 20–25% (Table 2, Fig. 4b).

Crystallomorphological analysis showed that all samples contain zircon of mainly H, L1, L4, S6, S7, S9, S15, and S25 types. According to the diagram (Belousova et al., 2006), H and L1 zircons are typical of S-type peraluminous granites; L4, of hybrid monzonites and alkaline granites; S6 and S7, of calc-alkaline granites; S9, of contaminated subalkaline and alkaline granites; S15, of I-type subalkaline and alkaline granites; and S25, of I-type alkaline and tholeiitic granites. This analysis illustrates that zircons were derived from granitoids of different types. All samples demonstrate the sharp predominance (32–42%) of euhedral zircons typical of peraluminous granites (H and L1).

U/Pb Zircon Dating by Laser Ablation (LA-ICP-MS)

Analyses were carried out at the University of California Santa Cruz LA-ICP-MS laboratory using an Element XR high-resolution magnetic-sector ICP-MS and a Photon Machines Analyte.H 193 nm eximer laser equipped with a Helex 2-volume laser ablation

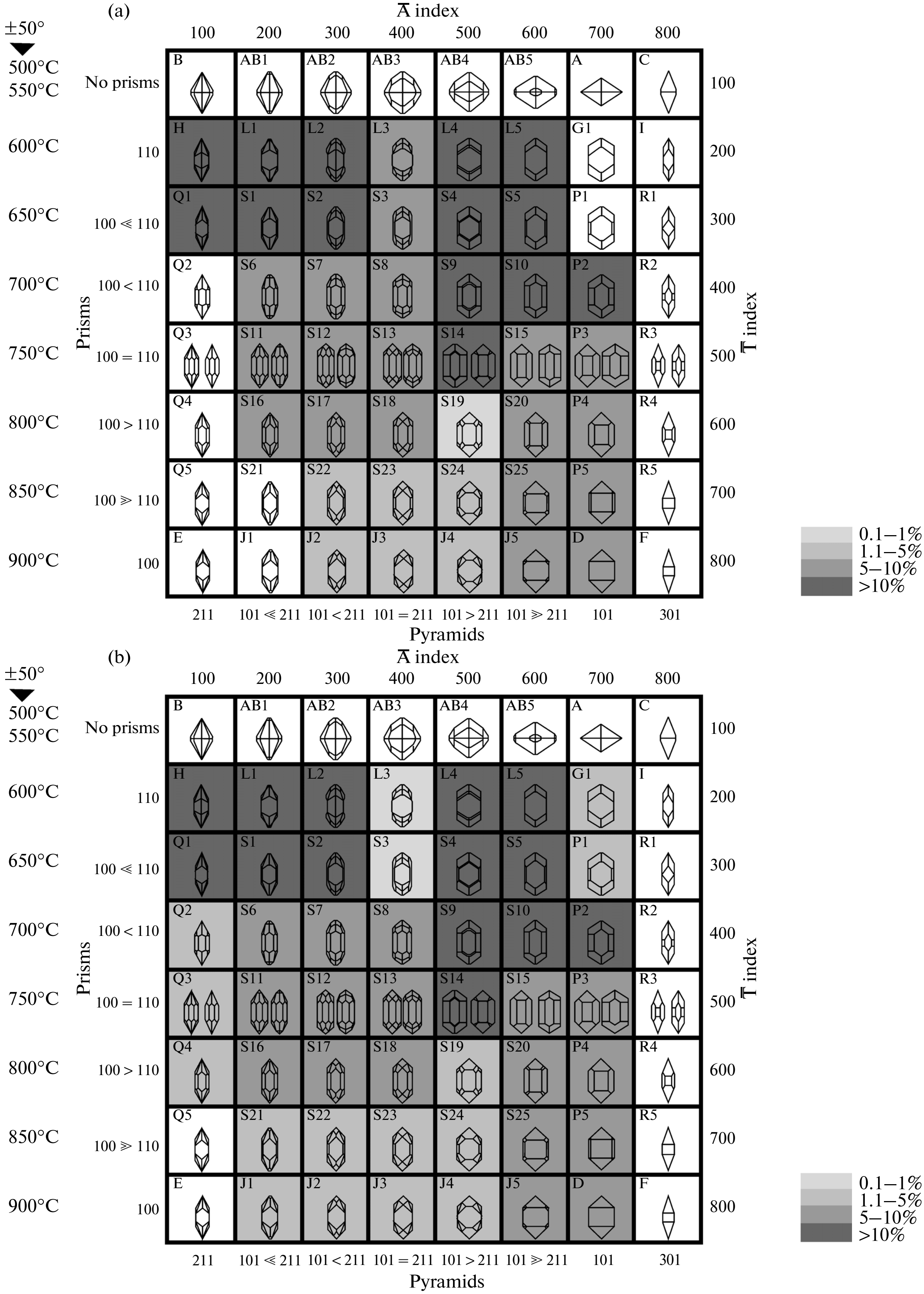
(a)
A̅ index
100 200 300 400 500 600 700 800
±50°
500°C
550°C
600°C
650°C
700°C
750°C
800°C
850°C
900°C
Prisms
No prisms
110
100 ≪ 110
100 < 110
100 = 110
100 > 110
100 ≫ 110
100
B AB1 AB2 AB3 AB4 AB5 A C
H L1 L2 L3 L4 L5 G1 I
Q1 S1 S2 S3 S4 S5 P1 R1
Q2 S6 S7 S8 S9 S10 P2 R2
Q3 S11 S12 S13 S14 S15 P3 R3
Q4 S16 S17 S18 S19 S20 P4 R4
Q5 S21 S22 S23 S24 S25 P5 R5
E J1 J2 J3 J4 J5 D F
T̅ index
100 200 300 400 500 600 700 800
211 101 ≪ 211 101 < 211 101 = 211 101 > 211 101 ≫ 211 101 301
Pyramids
0.1–1%
1.1–5%
5–10%
>10%
(b)
A̅ index
100 200 300 400 500 600 700 800
±50°
500°C
550°C
600°C
650°C
700°C
750°C
800°C
850°C
900°C
Prisms
No prisms
110
100 ≪ 110
100 < 110
100 = 110
100 > 110
100 ≫ 110
100
B AB1 AB2 AB3 AB4 AB5 A C
H L1 L2 L3 L4 L5 G1 I
Q1 S1 S2 S3 S4 S5 P1 R1
Q2 S6 S7 S8 S9 S10 P2 R2
Q3 S11 S12 S13 S14 S15 P3 R3
Q4 S16 S17 S18 S19 S20 P4 R4
Q5 S21 S22 S23 S24 S25 P5 R5
E J1 J2 J3 J4 J5 D F
T̅ index
100 200 300 400 500 600 700 800
211 101 ≪ 211 101 < 211 101 = 211 101 > 211 101 ≫ 211 101 301
Pyramids
0.1–1%
1.1–5%
5–10%
>10%

cell. Ablated aerosol was transported through 4-mm inner Teflon tubing. The ALTEX laser is energy stabilized at 4.5 mJ. The energy density control was provided by a user settable attenuator.

The grains of detrital zircon were mounted in rows on double-sided sticky tape using a mask cut from the tape backing film. Zircon standards SL2 (563 Ma; Gehrels et al., 2008) and Plesovice (337 Ma; Slama et al., 2008) were mounted at the center of the mount. Then, the grains were potted in a ring form using Struers Epofix epoxy resin. The solidified mount was cut off to the required size using a turning machine. The mount surface with zircon grains was successively polished with 1500 grit sandpaper, 9 and 3 μm Struers polishing compounds on a LaboPol lap wheel. Cathodoluminescence images were obtained at the Microanalytical Center of the Stanford University (http://shrimprg.stanford.edu) using a JEOL JSM 5600 scanning electron microscope with cathodoluminescence detector.

A series of four primary SL2 (Gehrels et al., 2008) and secondary Plesovice (Slama et al., 2008) standards were analyzed at the beginning and end of each seccion. Primary standard was analyzed after every fifth analysis of grains of unknown age and were paired with secondary standard after every tenth analysis. According to the measurement protocol, 15 secondary standard zircons were analyzed per 100 analyses to monitor the quality and accuracy of measurements. The obtained data were reduced using the Iolite add-ons for Igor Pro (Paton et al., 2010). It was taken that the exponential detrending algorithm based on the downhole fractionation of standards is more reliable than the linear regression technique, “ratio-of-means” or “mean-of-ratios” data reduction methodologies. In particular, we favor the detrending approach, because unknowns that exhibit different fractionation behavior support a temporal trend after down-hole correction, which leads to the higher standard deviation when signal is averaged. Thus, the accuracy is estimated as the difference between the ablation behavior of the standards and grains of unknown age.

Synchronization and the reproducible sample washout of the Helex-2 allow the automatic integration based on fixed time intervals without modifications for 90% of typical samples. Integration regions are resized if grain was burned through by laser, which is expressed in a sharp decrease of signal during laser operation, or spikes of ^{204}Pb are observed among the background values. Total ^{204}Pb backgrounds (Pb + Hg) usually account for ~300 ± 10 counts per second. Other than ^{204}Pb peaks related to the inclusions or high U content (high damage degree?), the average background signals are typically less than the established limit of detection of three times the standard deviations. For this reason, the ^{204}Pb correction was replaced by the 207-corrected ^{206}Pb/^{238}Pb age.

Grains of detrital zircon extracted from the core of Well Severnaya were dated by U/Pb LA-ICP-MS. One hundred grains were dated from each sample. The concordia (Wetherill, 1956) and Tera Wasserburg (Tera and Wasserburg, 1972) diagrams were plotted using ISOPLOT 3.0 (Ludwig, 2003) (Fig. 5). Calculations were made only for concordant grains (Figs. 5, 6). Zircon in all samples shows a wide age range (Fig. 6). The studied sandstones contain zircons of Mesozoic, Paleozoic, and Precambrian ages in different proportions (Fig. 6).

Grains with an age of 276.2 ± 1.4 Ma (±2σ, seven grains) are distinctly distinguished in sandstone (sample C2688, upper Anisian). This sample also contains zircon of the following age intervals: 280–300 and 320–360 Ma with clearly expressed peak at 343 Ma; 590–790 Ma and 590–790 Ma with main peak at 632 Ma (Fig. 6). No zircons older than 800 Ma were found in this sample.

Sample C2073 (upper Ladinian) contains a great amount (48) of discordant grains. The concordant ages of zircon are distributed over intervals (Ma): 240–250, 290–360, and 440–690. Zircon grains older than 700 Ma are rare. Insignificant peaks are noted at 1424 and 1540 Ma.

Sandstone (sample C1040) contains zircon with an age of 218.8 ± 6.4 Ma (±2σ, three grains), which is slightly younger than the sedimentation age determined by biostratigraphic methods (Upper Triassic, upper Carnian) (Preobrazhenskaya et al., 1985; Dypvik et al., 1998). This may be the reason for the revision of age of the given stratigraphic interval. The obtained data suggest that sedimentation in the Late Triassic (Norian) was accompanied by volcanism (and/or magmatism) in the surrounding structures. Zircon ages are grouped into following age intervals: 220–245 Ma with clearly expressed peak at 233 Ma; 250–490 Ma with peaks at 259, 309, 345, 400, and 460 Ma (Fig. 6). Zircon older than 500 Ma does not define statistically significant peaks, except for the peak at 791 Ma.

A significant amount of zircon found in sample C633 has the Norian age, which is presumably close to the formation time of sandstones. The following age intervals are distinguished: 220–235, 270–280, and 310–315 Ma. There is a clearly expressed peak at 490–540 Na with maximum at 511 Ma (Fig. 6). Zircons older than 600 Ma do not define the statistically significant peaks, except for the peak at 1460–1530 Ma.

Fig. 4. Morphological classification of zircon crystals (Pupin, 1980). Shown is the content of detrital zircon of different morphological types in sandstone samples: (a) C2688, (b) C633 (Table 2). Index A is the Al/(Na + K) ratio controlling the development of zircon pyramids, index T shows the temperature affecting the development of zircon prism.

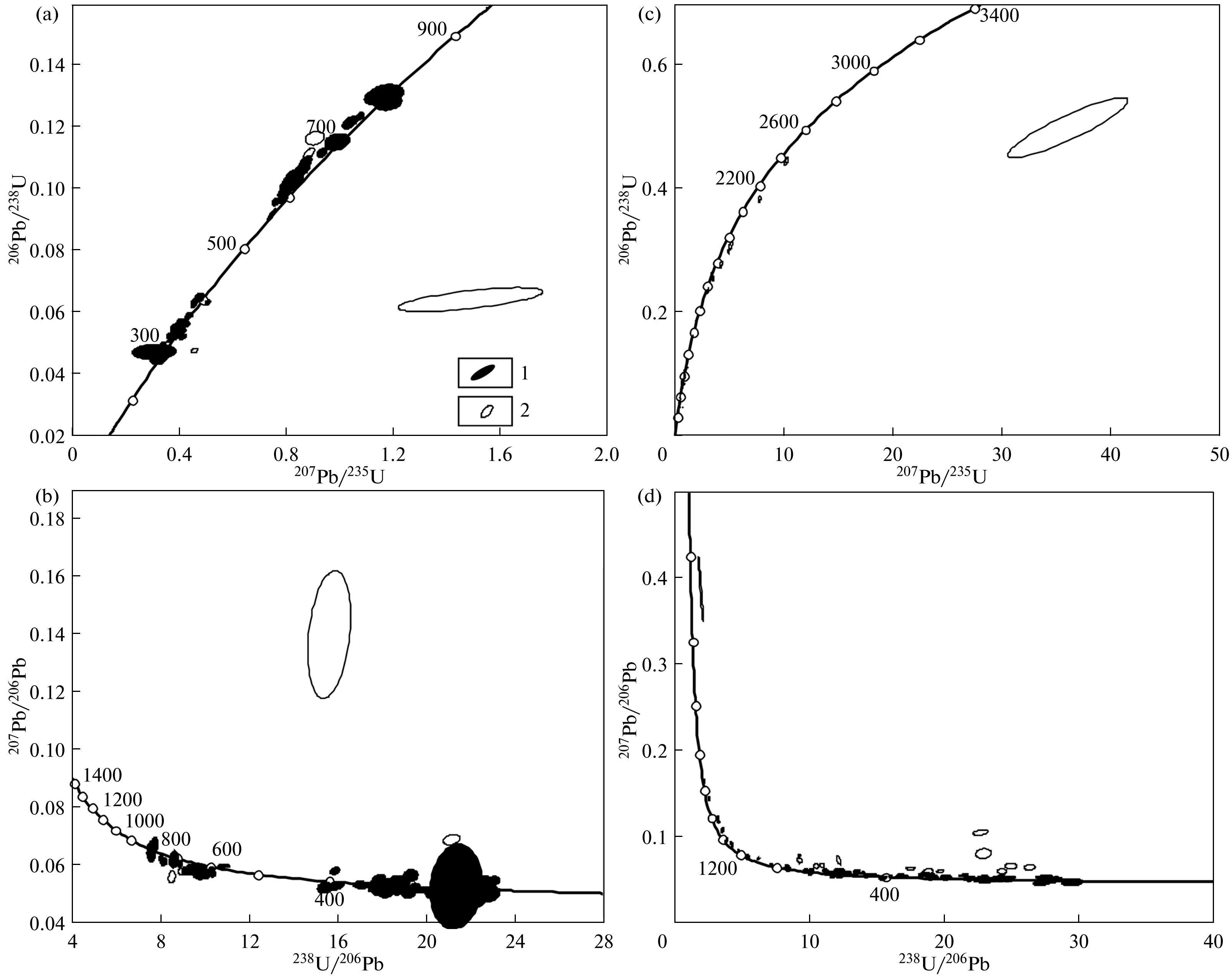

Fig. 5. Isotope diagrams for samples. C2688: (a) concordia, (b) Tera—Wasserburg); C633: (c) concordia, (d) Tera-Wasserburg. Error ellipse size is given in ±2σ. (1) Concordant determinations, (2) discordant determinations.

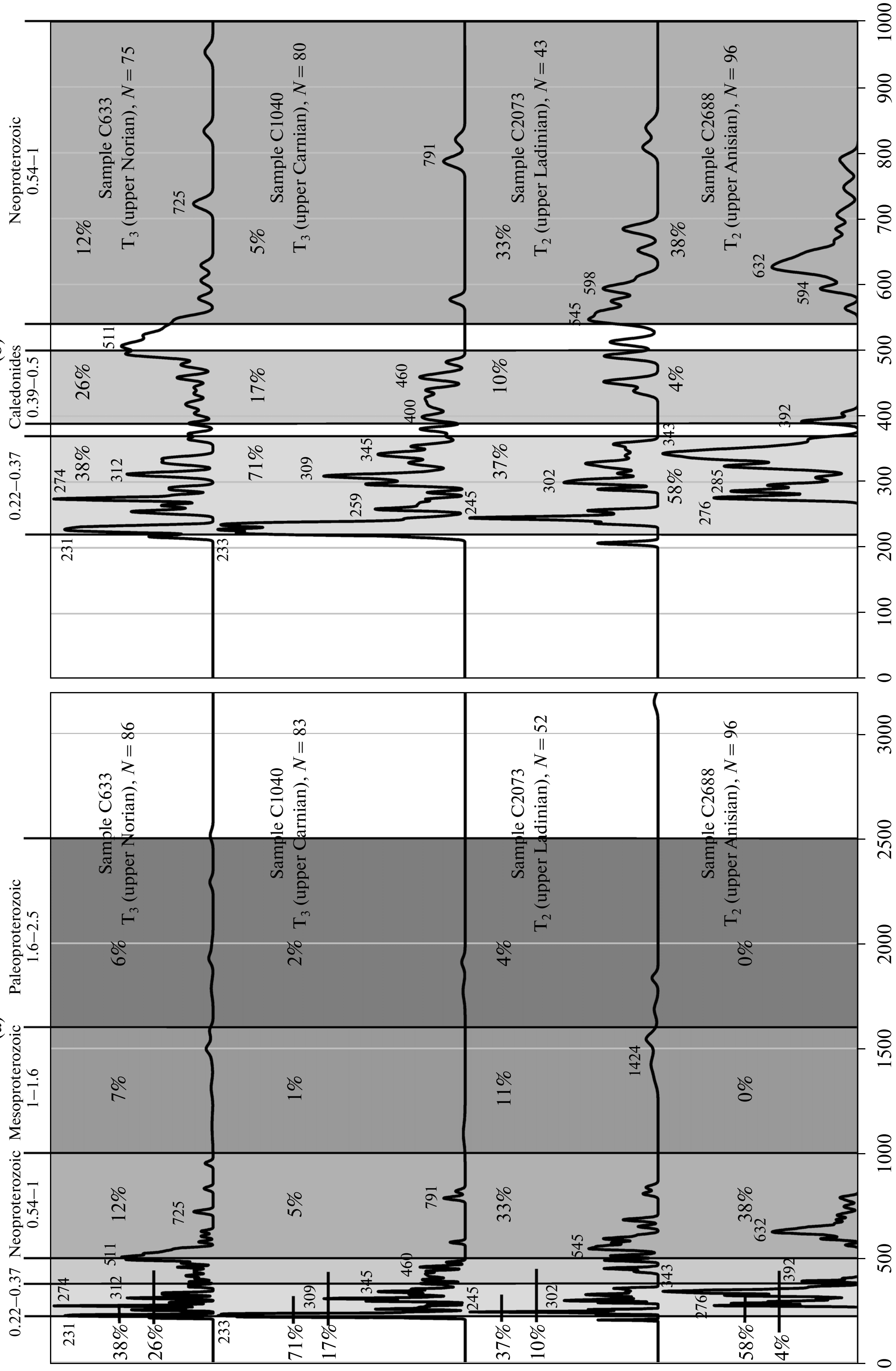

Fig. 6. Normalized probability density (frequency) distribution diagrams for detrital zircon in samples from Well Severnaya in coordinates: (a) 0–3200 Ma, (b) 0–1000 Ma. N is the number of dated concordant values. Percents denote the number of grains of the given age interval in the total number of dated grains.

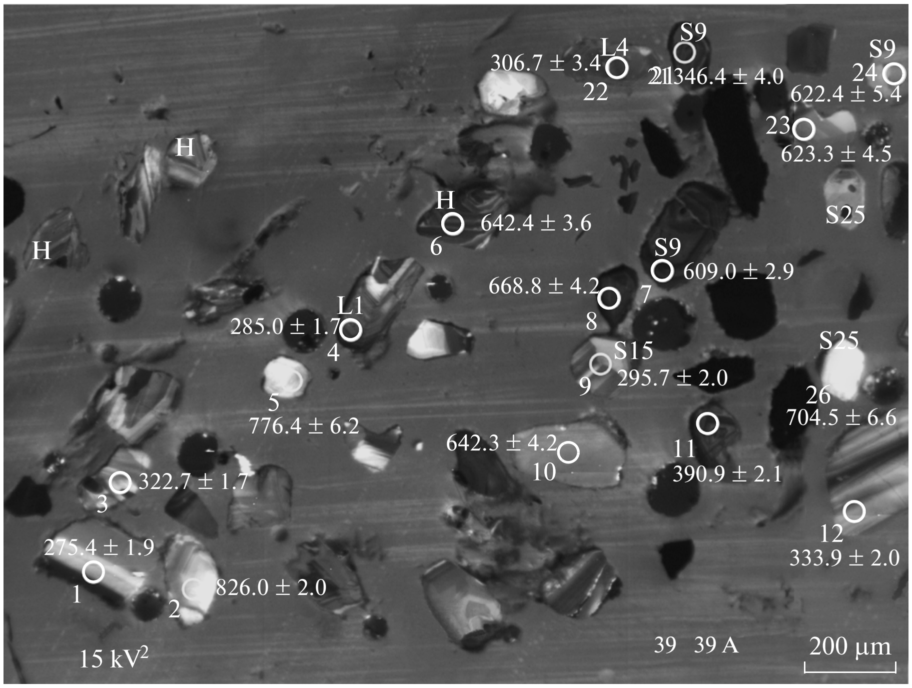

Fig. 7. Cathodoluminescence images of the detrital zircon from sample C2688. Circles show the concordant ages, numeral denotes the number of dated zircon. Age is given with error ±1σ. Morphological types of crystals are given after (Pupin, 1980).

Comparison of the Zircon Age and Morphology

Morphology of detrital zircon was also analyzed using images obtained by cathodoluminescence detector mounted on a JEOL JSM 5600 scanning electron microscope (Fig. 7). There is no clear correlation between morphology and age of zircons. For instance, euhedral grains, which are dominant in the studied samples and typical of peraluminous granites (H and L1) (Belousova et al., 2006), have a wide age range (Fig. 8).

PROVENANCE EVOLUTION AND PALEOGEOGRAPHIC RECONSTRUCTIONS

The studied samples are sharply dominated by Paleozoic and Mesozoic zircons, with a significant amount of Neoproterozoic zircons, insignificant Meso- and Neoproterozoic zircons, and practical absence of Archean zircons.

Samples from Well Severnaya (Franz Josef Land Archipelago) contain only two Archean grains (>2.5 Ga), thus indicating that Archean provenances played no role in the accumulation of Triassic rocks in this region.

Zircons of the Paleo- and Mesoproterozoic (2.5–1.0 Ga) age are absent in the Anisian sandstones (sample C2688). They appear in significant amount (15%) only in the Ladinian rocks (sample C2073) (1.8–1.6 and 1.4–1.5 Ga). The role of these sources becomes weaker (3%) in the Carnian (sample 1040) and again increases in the Norian (sample 633, 13%) (Fig. 6). The Paleo- and Mesoproterozoic zircons were presumably derived from the East European Craton (Baltica) (Patchett and Kuovo, 1986; Bogdanova et al., 2008; Bingem and Soll, 2009), although zircon of this age interval is also known in northern Laurentia (Heinriksen et al., 2000). Note that Baltica is a more preferable provenance, because zircons with ages of 1.48–1.64 Ga found in samples from Well Severnaya are absent in Laurentia.

The Grenvillian (1.14–0.9 Ga) provenances did not affect the Triassic sedimentation, because samples from Well Severnaya contain only three zircons of this age (Bogdanova et al., 2008; Lorenz et al., 2012).

The Neoproterozoic (1.0–0.54 Ga) zircons were delivered to sediments in significant amounts in the Anisian (0.8–0.56 Ga) (38%) and Ladinian (0.84–0.54 Ga) (33%). They factually disappeared in the Carnian (5%) and again appeared in the Norian (12%). Sources of the Neoproterozoic zircon are widespread in the surrounding structures of the Barents Sea, along the eastern front of the Polar Urals, and in Novaya Zemlya, Scandinavia, and Svalbard (Kuznetsov et al., 2010). Neoproterozoic magmatic rocks related to the Timan orogeny served as significant source of zircon of this age in the Barents Sea region (Larionov et al., 2004; Pease, 2011). Sources with an age of 630–615 Ma are known in the central Taimyr (Pease and Vernikovsky, 2000). Vendian detrital zircons (650 Ma) were found in the northern Taimyr (Pease and Scott, 2009). Granitoids of this age

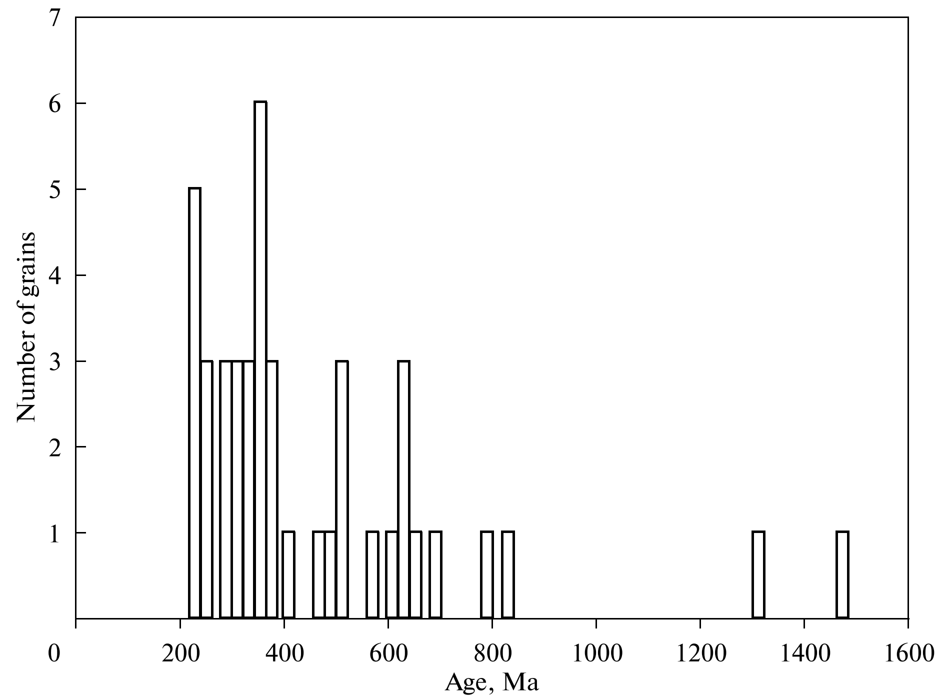

Fig. 8. Bar charts for the detrital zircon of morphological types H and L1 (Pupin, 1980) that are typical of peraluminous granites in samples from Well Severnaya (Franz Josef Land Archipelago).

are also typical of the western Siberian Craton (Vernikovsky et al., 2003). We believe that the main sources of the Neoproterozoic zircon in the studied samples were the Polar Urals and, possibly, Novaya Zemlya and Taimyr.

The amount of zircon related to the Caledonian (500–390 Ma) stage systematically increases from the Anisian (400–390 Ma, 4%), Ladinian (500–440 Ma, 10%), Carnian (480–390 Ma, 17%) to the Norian (500–390 Ma, 26%). Thus, the Caledonian complexes were gradually exhumed by the beginning of the Middle Triassic to play a significant role during the Late Triassic erosion. Zircons with age of 500–480 Ma were presumably derived from eroded magmatic rocks that were formed at the final stage of the Timan Orogeny (Gee et al., 2000; Kuznetsov et al., 2007) or during rifting of the Ordovician passive margin of the Urals (Puchkov, 1997). Magmatic and metamorphic rocks formed in the Caledonian time are known on the Severnaya Zemlya Archipelago (490–410 Ma) (Lorenz et al., 2007) and Svalbard (470–410 Ma) (Myhre et al., 2008; Petterson et al., 2010).

Zircon dated within 370–320 Ma forms the most significant peak in all samples: Anisian (370–270 Ma, 58%), Ladinian (360–270 and 270–240 Ma, 37%), Carnian (370–270 Ma and 270–220 Ma, 71%), and Norian (370–270 Ma and 270–220 Ma, 38%). Zircon of the age interval from 370 to 300 Ma and, possibly, to 270 Ma is related to the Hercynian (Uralian) magmatism, the manifestations of which are known in the Polar Urals and Taimyr (Zonenshain et al., 1990; Brown et al., 2006; Pease, 2011). The youngest zircons (250–220 Ma) were presumably derived from magmatic and volcanic rocks that are related to the Siberian plume and known in Taimyr (Vernikovsky et al., 2003; Walderhaug et al., 2005) and Siberian Craton (Reichow et al., 2009), as well as in boreholes in northern West Siberia (Saraev et al., 2009; Nikishin et al., 2011).

Results of the dating of detrital zircon from Well Severnaya provide insight into the evolution of provenances for the northern part of the Barents Sea in the Middle–Late Triassic.

The Middle Triassic (upper Anisian) clastic material was mainly delivered from the Hercynian structures of the Polar Urals. These sources fed the basin with zircons of 370–270 Ma. Sources of Neoproterozoic zircon (800–560 Ma), second in significance, are inferred to be rocks of the eastern front of the Polar Urals, Novaya Zemlya, and northern and central Taimyr. Clastic material was delivered from the south and southeast.

By the end of the Middle Triassic (upper Ladinian), the Hercynian (360–270 Ma) and Neoproterozoic (840–540 Ma) rocks remained the main zircon sources, but their contribution decreased. Erosion of the Permo-Triassic magmatic and volcanic rocks (250–220 Ma) introduced a new source area. Transfer from the Caledonian structures increased, and zircon grains with age of 500–440 Ma were derived from both the south (Late Timanides, Polar Urals) and east (Severnaya Zemlya Archipelago). Transportation from the west (Svalbard Archipelago) is less probable. At the end of the Middle Triassic, the Paleo- and Mesoproterozoic rocks of the East European Craton (Baltica) began to erode.

The beginning of the Late Triassic (upper Carnian) is marked by increasing erosion of magmatic rocks related to the Siberian plume (250–220 Ma) and a detrital supply from the Hercynian (370–270 Ma) and Caledonian (480–390 Ma) structures. Paleo- Meso-, and Neoproterozoic rocks were virtually not eroded.

The end of Triassic (upper Norian) was marked by decrease in erosion of rocks with age of 250–220 Ma and 370–270 Ma (Hercynian sources) and increase in the contribution of Caledonian (500–390 Ma) complexes. Erosion of the Paleo-, Meso-, and Neoproterozoic rocks was intensified.

Thus, the main sources of clastic material in the North Barents Sea sedimentary basin in the Middle—Late Triassic were structures of the Uralian fold belt, with a lesser contribution of the East European Craton, Baltica, Timanides, Taimyr, and Siberian traps. The material was presumably delivered mainly from the south and southeast. The contribution of the Neoproterozoic sources systematically decreased, while the role of the Caledonian sources increased from the beginning of the Middle to the end of the Late Triassic. The obtained data indicate that terrigenous material carried from the Uralian fold belt reached the Franz Josef Land Archipelago no later than in the Middle Triassic and was transferred to Svalbard only in the Late Triassic (Riis et al., 2008; Bue et al., 2011; Bue and Andersen, 2013). Triassic sediments of the Franz Josef Land Archipelago were deposited in a single North Barents Basin, and their formation was not related to the evolution of the Svedrup Basin.

Paleogeographic reconstructions for the Barents Sea region were previously based mainly on the lithological, mineralogical, biostratigraphic, and seismic data (Ronkina and Vishnevskaya, 1981, 1982; Pchelina, 1985; Mørk, 1999; Kosteva, 2004; Petrov et al., 2008; Basov et al., 2009). It was proposed that the Franz Josef Land Basin in the Triassic was fed from the northern Mid-Arctic land (Lomonosov Ridge) (Ronkina and Vishnevskaya, 1981, 1982; Kosteva, 2004). However, this conclusion is not confirmed by our data. Their comprehensive analysis showed that detrital material was transported to the Barents Sea Basin by the Severnaya Zemlya mountain system, as well as Novaya Zemlya–Uralian, Baltic, and West Svalbard paleolands (Basov et al., 2009). The obtained U–Pb data on detrital zircon are well-consistent with these paleogeographic reconstructions (Basov et al., 2009). In recent years, the paleogeographic reconstructions for Arctic regions were verified by the U/Pb age data on detrital zircon (Miller et al., 2006; Pease et al., 2007; Petrov, 2010; Bue et al., 2011; Omma et al., 2012; Miller et al., 2013; Bue and Andersen, 2013). These data together with the results presented in this paper allowed us to significantly specify the provenances of Triassic rocks in the Barents Sea region (Pease et al., 2007; Petrov, 2010; Bue et al., 2011; Bue and Nadersen, 2013). Thus, the U/Pb dating of detrital zircon bears important information on provenances and provides the correction of regional paleogeographic reconstructions.

CONCLUSIONS

(1) Morphological analysis of detrital zircon crystals from four core samples of the Triassic rocks recovered by Well Severnaya in the Franz Josef Land Archipelago showed that the main source rocks were peraluminous granites in association with calc-alkaline, subalkaline, and alkaline granitoids.

(2) The LA-ICP-MS U/Pb data on detrital zircons (400 age determinations) were used to decipher the evolution of provenance for the Barents Sea region in the Middle—Late Triassic. At the beginning of the Middle Triassic, the main sources of clastic material were Hercynian structures of the Urals. Sources of the Neoproterozoic zircon, second in significance, were the complexes of the Polar Urals. It could also be transported from Novaya Zemlya and northern and central areas of Taimyr. The clastic material came from the south and southeast. By the end of the Middle Triassic, the Hercynian and Neoproterozoic provenances remained the main sources of clastic material. Magmatic rocks presumably related to the Siberian plume (250–220 Ma) and Paleo- and Mesoproterozoic rocks of the East European Craton (Baltica) began to erode. Transport of zircon from the typical Caledonian structures increased. Its possible sources were late Timanides, Polar Urals, and Severnaya Zemlya. At the beginning of the Late Triassic, rocks related to the Siberian plume, Hercynian and Caledonian structures continued to supply clastic material, while the transport from Paleo-, Meso-, and Neoproterozoic structures virtually ceased. By the end of the Triassic, the erosion of Siberian traps and Hercynian rocks decreased, giving way to the Caledonian complexes, as well as Paleo-, Meso-, and Neoproterozoic structures.

(3) The main sources of clastic material for the North Barents Sea sedimentary basin in the Middle–Late Triassic were structures of the Uralian fold belt. Terrigenous material was presumably also supplied from the East European Craton (Baltica), Timanides, Taimyr, and rocks of the Siberian plume. The material was mainly delivered from the south and southeast. Influence of the Neoproterozoic sources systematically decreased, while the role of the Caledonian sources increased from the beginning of the Middle to the end of the Late Triassic. The U/Pb zircon dating shows that sediments derived from the Uralian fold belt reached the Franz Josef Land Archipelago by the Middle Triassic and accumulated in a single northern Barents Sea Basin.

ACKNOWLEDGMENTS

We are grateful to I.S. Ipat'eva (Geological Institute, Moscow) for help in obtaining and processing data used in the paper. A.V. Maslov is thanked for comments, which greatly improved our manuscript.

This work was financially supported by the Norwegian Petroleum Directorate, the Earth Science Division of the Russian Academy of Sciences (program nos. 4 and 6), and the Russian Foundation for Basic Research (project no. 14-05-93092 Norw_a).

REFERENCES

Basov, V.A., Vasilenko, L.V., Viskunova, K.G., et al., Evolution of sedimentation settings in the Barents–Severnaya Kara paleobasin in the Phanerozoic. *Geol. Teor. Prakt.*, 2009, vol. 4, no. 1. http://www.ngtp.ru/rub/2/3_2009.pdf

Belousova, E.A., Griffin, W.L., and O'Reily, S.Y., Zircon crystal morphology, trace element signatures and Hf isotope composition as a tool for petrogenetic modelling: examples from Eastern Australian granitoids, *J. Petrol.*, 2006, vol. 47, no. 2, pp. 329–353.

Bingen, B. and Soll, A., Geochronology of magmatism in the Caledonian and Sveconorwegian belts of Baltica: synopsis for detrital zircon provenance studies, *Norw. J. Geol.,* 2009, vol. 89, pp. 267–290.

Bogdanova, S.V., Bingen, B., Gorbatschev, R., et al., The East European Craton (Baltica) before and during the assembly of Rodinia, *Precambrian Res.*, 2008, vol. 160, nos. 1/2, pp. 23–45.

Bro, E.G., Pchelina, T.M., Preobrazhenskaya, E.N., et al., Sedimentary cover of the Barents Sea shelf based on parametric drilling on islands, in *Problemy neftegazonosnosti Mirovogo okeana* (Problems of petroleum Potential in the World Ocean), Moscow: Nauka, 1989, pp. 191–197.

Brown, D., Puchkov, V., Alvarez-Marron, J., et al., Tectonic processes in the Southern and Middle Urals: an overview, in *European Lithosphere Dynamics*, London: Geol. Soc. Mem., 2006, pp. 407–419.

Bue E.P., Andersen A. Constraining depositional models in the Barents Sea region using detrital zircon U-Pb data from Mesozoic sediments in Svalbard, in *Sediment Provenance Studies in Hydrocarbon Exploration and Production*, London: Geol. Soc. London, 2013 (in press).

Bue, E.P., Andersen, A., Andersen, T., and Solbakken, R.T., Provenance of Mesozoic sediments from Svalbard based on LA-Mc-ICPMS analyses of clastic zircons: Preliminary results, 2011. ftp://ftp.ngu.no/pub/NGF_Wintermeeting/Til%20Hans%20Arne/EBCE/EBCE3+6/PGE3O_Bue_Edina_Pozer.pdf

Bugge, T. and Fanavoll, S., The Svalis Dome, Barents Sea—a geological playground for shallow stratigraphic drilling, *First Break*, 1995, vol. 13, no. 6, pp. 237–251.

Dypvik, H., Sokolov, A., Pcelina, T., et al., The Triassic succession of the Franz Josef Land, stratigraphy and sedimentology of three wells from Alexandra, Hayes and Graham Bell Islands. Geological aspects of the Franz Josef Land and the northernmost Barents Sea, in *The Northern Barents Sea Geotraverse. Meddelelser no. 151*, Oslo: Norsk Polarinst., 1998.

Gee, D.G., Beliakova, L., Pease, V., et al., New single zircon (Pb-evaporation) ages from Vendian intrusions in the basement beneath the Pechora Basin, northeastern Baltica, *Polarforschung*, 2000, vol. 68, p. 161–170.11.

Gehrels, G., Detrital zircon U-Pb geochronology: current methods and new opportunities, *Recent Advances in Tectonics of Sedimentary Basins*, Busby, C. and Azor, A., Eds., Wiley-Blackwell 2011, pp. 47–62.

Gehrels, G.E., Valencia, V., and Ruiz, J., Enhanced precision, accuracy, efficiency, and spatial resolution of U-Pb ages by laser ablation-multicollector-inductively coupled plasma-mass spectrometry, *Geochem., Geophys., Geosystems*, 2008, vol. 9, p. Q03017. doi:10.1029/2007GC001805.

Gramberg, I.S., Shkola, I.V., Bro, E.G., et al., Parametric boreholes on islands in the Barents and Kara seas, *Sov. Geol.*, 1985, no. 1, pp. 95–98.

Henriksen, N., Higgins, A.K., Kalsbeek, F., and Pulvertaft, T.C.R., Greenland from Archean to Quaternary, *Geol. Surv. Denmark Greenland Bull.*, 2000, no. 185, pp. 2–12.

Kosteva, N.N., The sources of denudation for the Barents Sea Mesozoic sedimentary provinces, *Arctic Geology, Energy Resources and Environmental Challenges (NGF Abstr. Proc.)*, 2004, no. 2, pp. 74–75.

Kuznetsov, N.B., Soboleva, A.A., Udoratina, O.V., et al., Pre-Ordovician tectonic evolution and volcano-plutonic associations of the Timanides and northern Pre-Uralides, northeast part of the East European Craton, *Gondwana Res.*, 2007, vol. 12, pp. 305–323.

Kuznetsov, N.B., Natapov, L.M., Belousova, E.A., et al., Geochronological, geochemical and isotopic study of detrital zircon suites from late Neoproterozoic clastic strata along the NE margin of the East European Craton: implications for plate tectonic models, *Gondwana Res.*, 2010, vol. 17, pp. 583–601.

Larionov, A.N., Andreichev, V.A., and Gee, D.G., The Vendian alkaline igneous suite of northern Timan: ion microprobe U-Pb zircon ages of gabbros and syenite, in *The Neoproterozoic Timanide Orogen of Eastern Baltica*, London: Geol. Soc. Mem., 2004.

Lorenz, H., Gee, D.G., and Whitehouse, M.J., New geochronological data on Paleozoic igneous activity and deformation in the Severnaya Zemlya Archipelago, Russia, and implications for the development of the Eurasian Arctic margin, *Geol. Mag.*, 2007, vol. 144, pp. 105–125.

Lorenz, H., Gee, D.G., Larionov, A.N., and Majka, J., The Grenville-Sveconorwegian orogen in the high Arctic, *Geol. Mag.*, 2012, vol. 149, no. 05, pp. 875–891. doi:10.1017/S0016756811001130

Ludwig, K.R., *User's manual for Isoplot 3.0: A geochronological toolkit for Microsoft Excel*, Berkeley: Geochron. Center. Spec. Publ. 4, 2003.

Miller, E.L., Toro, J., Gehrels, G., et al., New insights into Arctic paleogeography and tectonics from U-Pb detrital zircon geochronology, *Tectonics*, 2006, vol. 25, p. TC3013. doi: 10.1029/2005TC001830.

Miller, E.L., Soloviev, A.V., Prokopiev, A.V., et al., Triassic river systems and the paleo-Pacific margin of northwestern Pangea, *Gondwana Res.*, 2013, vol. 23, no. 4. pp. 1631-11645. http://dx.doi.org/10.1016/j.gr.2012.08.015.

Mørk, M.B.E., Compositional variations and provenance of Triassic sandstones from the Barents shelf, *J. Sedim. Res.*, 1999, vol. 69, no. 3, pp. 690–710.

Myhre, P.I., Corfu, F., and Andresen, A., Caledonian anatexis of Grenvillian crust: a U-Pb study of Albert I Land, NW Svalbard, *Norw. J. Geol.*, 2008, vol. 89, pp. 173– 91.

Nikishin, V.A., Malyshev, N.A., Nikishin, A.M., and Obmetko, V.V., Late Permian–Triassic system of rifts in the South Kara sedimentary basin, *Mosc. Univ. Geol. Bull.*, 2011, no. 6, pp. 377–384.

Omma, J.E., Pease, V., and Scott, R.A., U-Pb SIMS zircon geochronology of Triassic and Jurassic sandstones on northwestern Heiberg Island, northern Sverdrup Basin, Arctic Canada, in *Arctic Petroleum Geology,* London: Geol. Soc. Mem., 2011.

Patchett, J. and Kuovo, O., Origin of continental crust of 1.9–1.7 Ga age: Nd isotopes and U-Pb zircon ages in the Svecokarelian terrain of South Finland, *Contrib. Mineral. Petrol.*, 1986, vol. 92, pp. 1–12.

Paton, C., Woodhead, J.D., Hellstrom, J.C., et al., Improved laser ablation U-Pb zircon geochronology through robust downhole fractionation correction, *Geochem. Geophys. Geosyst.*, 2010, vol. 11.

Pchelina, T.M., History of Triassic sedimentation in Spitsbergen and the adjacent shelf, in *Stratigrafiya i paleontologiya mezozoiskikh osadochnykh basseinov Severa SSSR* (Stratigraphy and Paleontology of Mesozoic Sedimentary Basins in the northern Soviet Union), Leningrad: Sevmorgeologiya, 1985, pp. 135–152.

Pease, V., Eurasian orogens and Arctic tectonics: an overview, in *Arctic Petroleum Geology*, London: Geol. Soc. Mem., 2011.

Pease, V. and Scott, R.A., Crustal affinities in the Arctic Uralides, northern Russia: significance of detrital zircon ages from Neoproterozoic and Palaeozoic sediments in Novaya Zemlya and Taimyr, *J. Geol. Soc. London*, 2009, vol. 166, pp. 1–10.

Pease, V. and Vernikovsky, V., The tectono-magmatic evolution of the Taimyr Peninsula: further constraints from new ion-microprobe data, *Polarforsch.*, 2000, vol. 68, pp. 171–178.

Pease, V., Kosteva, N., Tebenkov, A., et al., U-Pb zircon provenance of Late Triassic sandstone from Franz Josef Land, *Abstr. Proc. Geol. Soc. Norway*, ICAM V, 2007.

Petrov, E.O., Formation conditions of Mesozoic rocks in the Barents Sea region, *Extended Abstract of PhD (Geol.-Miner.) Dissertation*, Moscow: MGU, 2010.

Petrov, O.V., Sobolev, N.N., Koren, T.N., et al., Palaeozoic and Early Mesozoic evolution of the East Barents and Kara Seas sedimentary basins, *Norsk Geol. Tiddsskrift*, 2008, vol. 88, no. 4, pp. 227–234.

Pettersson, C.H., Pease, V., and Frei, D., Detrital zircon - Pb ages of Silurian-Devonian sediments from NW Svalbard: A fragment of Avalonia and Laurentia?, *J. Geol. Soc. London,* 2010, vol. 167, pp. 1018–1032. doi: 10.1144/0016-76492010-062.

Preobrazhenskaya, E.N., Shkola, I.V., and Korchinskaya, M.V., Stratigraphy of Triassic sediments in the Franz Josef Land Archipelago (based on parametric drilling), in *Stratigrafiya i paleontologiya mezozoiskikh osadochnykh basseinov Severa SSSR* (Stratigraphy and Paleontology of Mesozoic Sedimentary Basins in the northern Soviet Union), Leningrad: Sevmorgeologiya, 1985, pp. 5–15.

Puchkov, V.N., Structure and geodynamics of the Uralian orogen. Orogeny through time, *Geol. Soc. London Spec. Publ.*, 1997, vol. 121, pp. 201–236.

Pupin, J.P., Zircon and granite petrology, *Contrib. Miner. Petr.*, 1980, vol. 73, pp. 207–220.

Reichow, M.K., Pringle, M.S., Al'mukhamedov, A.I., et al., The timing and extent of the eruption of the Siberian Traps large igneous province: implications for the end-Permian environmental crisis, *Earth Planet. Sci. Lett.,* 2009, vol. 277, pp. 9–20.

Riis, F., Lundschien, B.A., Hoy, T., et al., Evolution of the Triassic shelf in the northern Barents region, *Polar Res.*, 2008, vol. 27, pp. 318–337.

Ronkina, Z.Z. and Vishnevskaya, T.N., Mineralogical criteria for paleogeographic reconstructions of the Kara sedimentation basin in the Jurassic–Cretaceous, in *Litologiya i paleogeografiya Barentseva i Karskogo morei* (Lithology and Paleogeography of the Barents and Kara Seas), Leningrad: NIIGA, 1981, pp. 85–96.

Ronkina, Z.Z. and Vishnevskaya, T.N., Glaucophane in sedimentary sequences in the western Soviet Arctic, *Sov. Geol.*, 1982, no. 7, pp. 90–93.

Saraev, S.V., Baturina, T.P., Ponomarchuk, V.A., and Travin, A.V., Permo-Triassic volcanics in the Koltogor–Urengoi rift, West Siberian geosyncline, *Geol. Geofiz.*, 2009, vol. 50, no. 1, pp. 4–20.

Slama, J., Kosler, J., Condon, D.J., et al., Plesovice zircon—a new natural reference material for U-Pb and Hf isotopic microanalysis, *Chem. Geol.*, 2008, vol. 249, pp. 1–35.

Tera, F. and Wasserburg, G.J., U-Th-Pb systematics in three Apollo 14 basalts and the problem of initial Pb in lunar rocks, *Earth Planet. Sci. Lett.*, 1972, vol. 14, pp. 281–304.

Ustritskii, V.I., Triassic and Upper Permian Rocks in the Admiralteistvo Peninsula (Novaya Zemlya), in *Litologiya i paleogeografiya Barentseva i Karskogo morei* (Lithology and Paleogeography of the Barents and Kara Seas), Leningrad: NIIGA, 1981, pp. 55–65.

Vernikovsky, V.A., Pease, V.L., Vernikovskaya, A.E., et al., First report of early Triassic A-type granite and syenite intrusions from Taimyr: product of the northern Eurasian superplume?, *Lithos*, 2003a, vol. 66, pp. 23–36.

Vernikovsky, V.A., Vernikovskaya, A.E., Kotov, A.B., et al., Neoproterozoic accretion-collisional events on the western margin of the Siberian Craton: new geological and geochronological evidence from the Yenisey Ridge, *Tectonophysics*, 2003b, vol. 375, pp. 147–168.

Walderhaug, H.J., Eide, E.A., Scott, R.A., et al., Paleomagnetism and 40Ar/39Ar geochronology from the south Taimyr igneous complex, Arctic Russia: a Middle-Late Triassic magmatic pulse after Siberian flood-basalt volcanism, *Geophys. J. Int.,* 2005, vol. 163, pp. 501–517.

Wetherill, G.W., Discordant uranium-lead ages, *Trans. Am. Geophys.,* 1956, Union 37, pp. 320–326.

Zircon, in *Rev. Miner. Geochem.*, Hanchar, J.M., Ed., P.W.O. Hoskin, 2003.

Zonenshain, L.P., Kuzmin, M.I., and Natapov, L.M., Uralian foldbelt and foldbelts of the Northeast USSR, Taimyr and the Arctic. Geology of the USSR: a plate-tectonic synthesis, *Am. Geophys. Union. Geodyn. Ser.*, 1990, vol. 21, pp. 121–146.

Translated by M. Bogina